

Performance of UNS S41427 Supermartensitic Stainless Steel in hydrochloric acid with the addition of propargyl alcohol as corrosion inhibitor

ABSTRACT

The search for Oil & Gas has led to the exploration of wells at increasingly greater depths, which requires the materials used to possess specific characteristics to withstand severe conditions of temperature and pressure. In this context, the use of stainless steels has been growing compared to carbon steels, due to their superior resistance to corrosion. To address these limitations, a subclass known as supermartensitic stainless steels has emerged. These steels exhibit superior corrosion resistance compared to martensitic steels, although, under certain conditions, they remain susceptible to corrosion, particularly pitting, generalized corrosion, intergranular corrosion, and stress corrosion in acidic environments containing sulfides. The objective of this study was to evaluate the corrosion behavior of the UNS S41427 supermartensitic stainless steel in a solution of hydrochloric acid at 10% and 15%, at temperatures of 30 °C, 45 °C, and 60 °C, over immersion times of 1 hour and 3 hours, and in concentrations of propargyl alcohol of 250 mg/L, 500 mg/L, and 1000 mg/L. The behavior of the material was also observed in the solution without the presence of the inhibitor. Gravimetric tests revealed that the corrosion rate increased with higher concentrations of HCl, temperature, and immersion time of the test specimen. Furthermore, the addition of propargyl alcohol resulted in a significant reduction in the corrosion rate under all analyzed conditions. The results indicated that the inhibitor's protection efficiency exceeded 80 - 90% in most experimental conditions, corroborating the initial expectations of the study.

Keywords: Supermartensitic stainless steel, corrosion, corrosion inhibitor, propargyl alcohol.

1. INTRODUCTION

Supermartensitic stainless steel, whose chemical composition is presented in Table 1, has a lower cost when compared to duplex and superduplex stainless steels and, in addition, has better characteristics related to weldability, toughness, resistance to generalized and localized corrosion in corrosive environments containing carbon dioxide (CO₂).

The term "super" is used to indicate the superior performance of this material in terms of corrosion resistance and weldability compared to martensitic steels. Because of these properties, supermartensitic stainless steel has been used in the manufacture of specialized equipment, components and tools for the acidizing process used to increase the productivity of oil and natural gas.

Table 1 – Chemical composition of UNS S41427 supermartensitic stainless steel (% by mass, Fe in balance).

Material,%	C	Mn	Cr	Ni	Mo	Si	V	S	P	N	Fe
UNS S41427	0.016	0.35	12.16	5.40	1.95	0.20	0.16	0.002	0.01	0.012	Bal.

In this acidification process analyzed in oil production, a carbon steel column was used, as shown in the diagram presented in Fig. 1, where the supermartensitic stainless steel inside the carbon steel pipe represents valves, connections, pump rotors, etc.

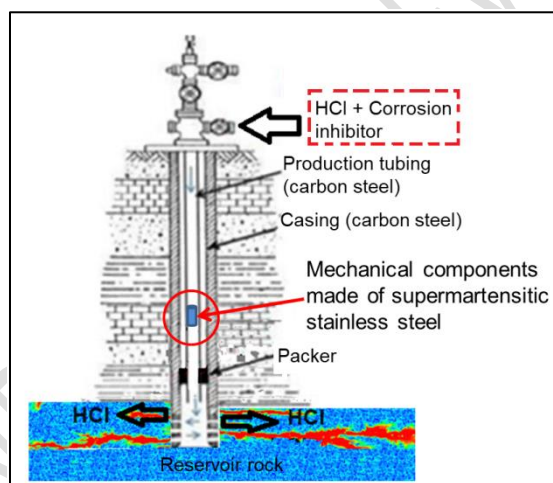


Fig.1. Hydrochloric acid injection scheme and mechanical components made of supermartensitic stainless steel

The chemical compositions of supermartensitic stainless steels are built on Fe-Cr-Ni-Mo with a high percentage of chromium associated with low carbon content (0.016%) and additions of nickel and molybdenum. The concentration of nitrogen and the additions of microalloys also contribute to the improvement of the properties of this stainless steel.

Nickel is one of those responsible for maintaining the purely martensitic structure without the formation of ferrite-delta, which is responsible for the appearance of cracks due to the sensitization phenomenon that occurs in these regions, when it is associated with the precipitation of chromium carbonitrides during the steel

tempering process. Molybdenum improves resistance to corrosion and sulfide stress corrosion [1-5].

As shown in Figure 1, the components manufactured with supermartensitic stainless steel are subjected to the conditions imposed by the acidification process, which essentially consists of the injection of hydrochloric acid containing a corrosion inhibitor based on propargyl alcohol (2-propin-1-ol). propyn

The acidizing process in oil production comprises the injection of hydrochloric acid into the reservoir rock aiming at the reaction of the injected acid with the rock, thus allowing greater permeability of the passage of oil and gas and, consequently, increasing oil production. In these operations, in order to protect the carbon steel, along with hydrochloric acid, a corrosion inhibitor is also added [6-10].

Commercial oil deposits are most frequently found in reservoir rocks formed by sedimentary rocks, mainly sandstones and limestones. Existing fractures also influence stimulation, since they occur at random intervals and sizes, depending on the type of rock. The chemical attack on the rock depends on the diffusion of the acid in the pores of the matrix rock, either by natural pathways or through induced fractures, which depends on the amount and concentration of the injected acid, the number and size of the existing fractures [11, 12].

Carbonate rocks are basically formed by limestones (CaCO_3) and dolomites ($\text{CaCO}_3.\text{MgCO}_3$). An oil well has a characteristic production profile. The decline in production may be due to damage to the porosity of the reservoir rock, preventing or restricting all or part of the flow of oil, gas and formation water over time. The acidification operation aims to restore production, that is, to increase the amount of oil produced by that well [13-15].

The reactions of hydrochloric acid with rocks containing limestone (CaCO_3) and dolomites ($\text{CaCO}_3.\text{MgCO}_3$) are presented below:



The present work aims to investigate the corrosive action of hydrochloric acid containing propargyl alcohol on UNS S41427 supermartensitic stainless steel.

2. MATERIALS AND METHODS

2.1 Materials testing

The UNS S41427 supermartensitic stainless steel coupons used in the gravimetric tests were fabricated with the following dimensions: 10.0 mm × 15.0 mm × 5.0 mm. The chemical composition of the UNS S41427 supermartensitic stainless steel is presented in Table 1. The coupon surfaces were polished with 100 to 600 grade sandpaper, cleaned with acetone, washed with bidistilled water and dried with hot air. The test coupons were weighed using a digital electronic balance.

The corrosive media used were 10% and 15% (by volume) HCl solutions of **high purity (% purity?)**. The concentrations of the corrosion inhibitor, propargyl alcohol (2-Propyn-ol-1) with 99% purity, were fixed at 250, 500 and 1,000 mg/L. The corrosion inhibitor choice and its concentrations are based on the authors' acidification experiments with HCl to ensure the integrity of materials such as carbon steel and special steels [16, 17].

2.2 Gravimetric test (mass loss) of coupons

The mass loss tests were performed out by immersing the supermartensitic stainless steel coupons in polyethylene bottles containing HCl solution with and without corrosion inhibitor and maintained in thermostatically controlled baths at temperatures of 30, 45 and 60°C (with an accuracy of 0.1°C), as shown in Fig. 2. The test times were set at 1 and 3 hours of exposure. After the experiments were completed, the coupons were removed from the corrosive medium, washed with bidistilled water and ethanol, and quickly dried with hot air. The coupons were then reweighed again to the nearest 0.0001 g according to ASTM G 31-72 standard [18].



Fig.2. Polyethylene bottles with coupons on thermostatic bath

The corrosion rate (CR) and the efficiency of each corrosion inhibitor (%E) were defined by the following expressions:

$$CR = \frac{W_o - W_f}{A} \quad \text{and} \quad E\% = \frac{W_a - W_i}{W_a} \times 100$$

Where:

Corrosion Rate = CR (unit) time in time in the unit per year or?);

Corrosion Inhibitor Efficiency = E %;

Wo and Wf are, respectively, the initial mass and the final mass of the coupon (units);

Wa and Wi are the weight loss of the coupon in the absence and presence of inhibitor;

S? = area (cm²).

3. RESULTS AND DISCUSSION

3.1 Gravimetric Test (mass loss) Results

3.1.1 Results of mass loss measurement of supermartensitic stainless steel coupons in hydrochloric acid without corrosion inhibitor

The results of the mass loss tests, carried out with a solution of 10% and 15% (by volume) of hydrochloric acid, in the absence of propargyl alcohol (corrosion inhibitor), at temperatures of 30°C, 45°C and 60°C are shown in the graphs in Fig. 3 and 4.

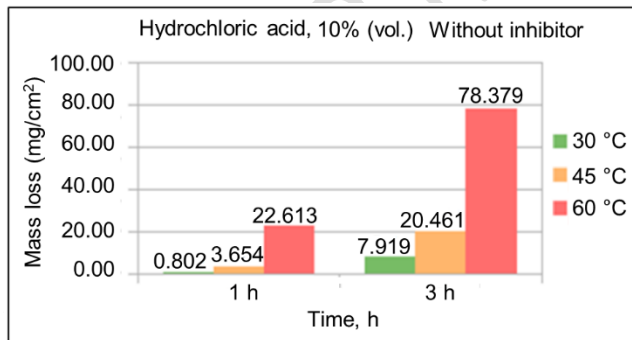


Fig. 3. Mass loss tests of supermartensitic stainless steel in 10% HCl solution without corrosion inhibitor (use editable chart, remove heading)

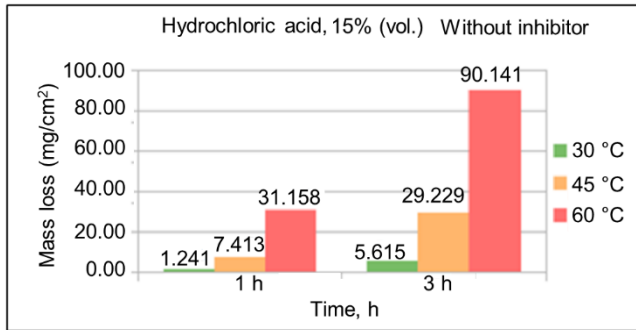


Fig. 4. Mass loss tests of supermartensitic stainless steel in 15 % HCl solution without corrosion inhibitor (Same as in Fig. 3)

3.1.2 Results of mass loss measurement of supermartensitic stainless steel coupons in hydrochloric acid with 250 mg/L propargyl alcohol

The results of the mass loss assays, carried out with 10% and 15% hydrochloric acid solution (by volume), with the addition of 250 mg/L of propargyl alcohol, at temperatures of 30°C, 45°C and 60°C are shown in the graphs of Fig. 5 and 6.

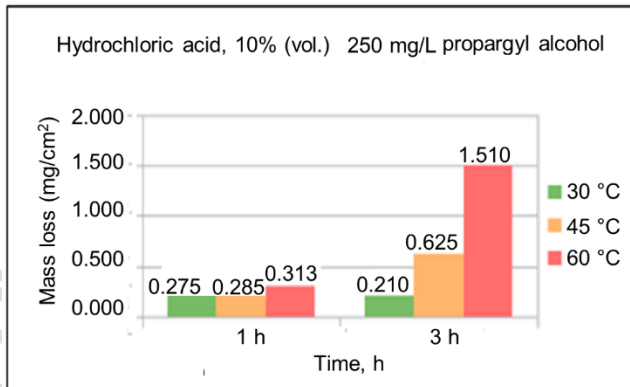


Fig. 5. Mass loss tests of supermartensitic stainless steel in 10 % HCl with the addition of 250 mg/L of propargyl alcohol (Same as in Fig. 3)

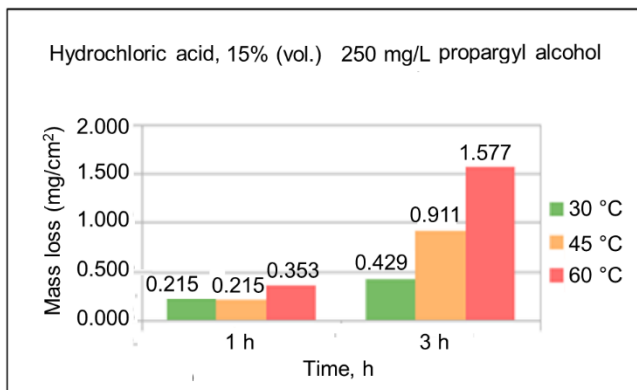


Fig. 6. Mass loss tests of supermartensitic stainless steel in 15 % HCl with the addition of 250 mg/L of propargyl alcohol (Same as in Fig. 3)

3.1.3 Results of mass loss measurement of supermartensitic stainless steel coupons in hydrochloric acid with 500 mg/L propargyl alcohol

The results of the mass loss assays, carried out with 10% and 15% hydrochloric acid solution (by volume), with the addition of 500 mg/L of propargyl alcohol (corrosion inhibitor), at temperatures of 30°C, 45°C and 60°C are shown in the graphs of Fig. 7 and 8.

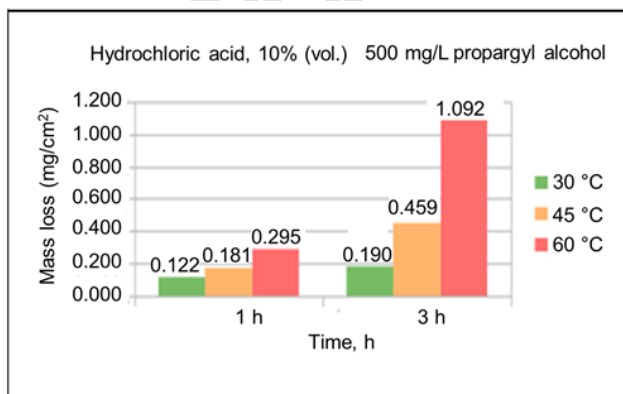


Fig. 7. Mass loss tests of supermartensitic stainless steel in 10 % HCl with the addition of 500 mg/L of propargyl alcohol (Same as in Fig. 3)

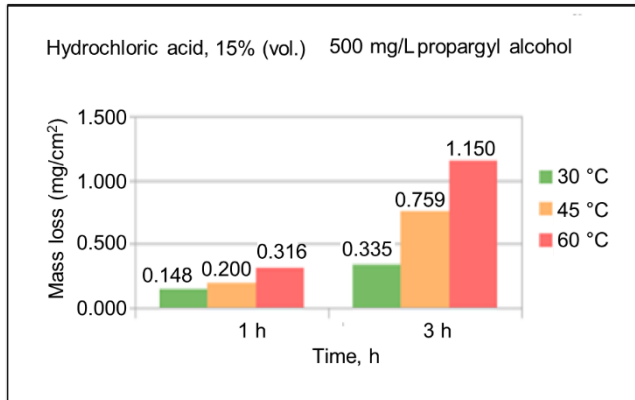


Fig. 8. Mass loss tests of supermartensitic stainless steel in 15 % HCl with the addition of 500 mg/L of propargyl alcohol (Same as in Fig. 3)

3.1.4 Results of mass loss measurement of supermartensitic stainless steel coupons in hydrochloric acid with 1000 mg/L propargyl alcohol

The results of the mass loss assays carried out with 10% and 15% hydrochloric acid (HCl) solution (by volume), with the addition of 1000 mg/L of propargyl alcohol, at temperatures of 30°C, 45°C and 60°C, are shown in the graph of Fig. 9 and 10.

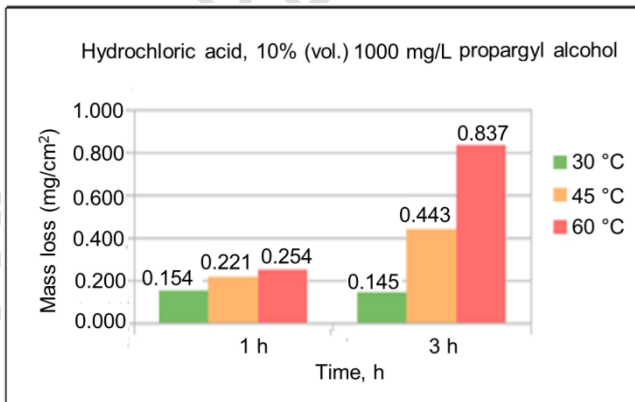


Fig. 9. Mass loss tests of supermartensitic stainless steel in 10 % HCl with the addition of 1000 mg/L of propargyl alcohol (Same as in Fig. 3)

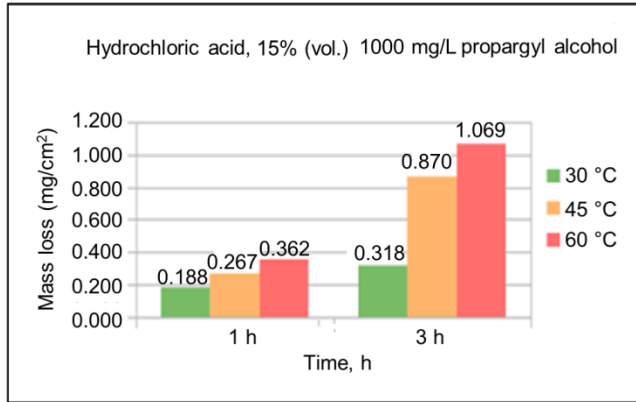


Fig. 10. Mass loss tests of supermartensitic stainless steel in 10 % HCl with the addition of 1000 mg/L of propargyl alcohol (Same as in Fig. 3)

3.1.5 Results of mass loss measurement of supermartensitic stainless steel coupons in hydrochloric acid (15 % vol.) with additions of 250, 500 and 1000 mg/L propargyl alcohol in 3 h

The logarithmic graph presented in Fig. 11 aims to summarize and compare in the most critical conditions (15 % HCl concentration and within 3 hours) that the coupons of supermartensitic stainless steel when submitted to mass loss tests, shows that the corrosion rate is high and the addition of propargyl alcohol promotes a significant reduction of this corrosion rate.

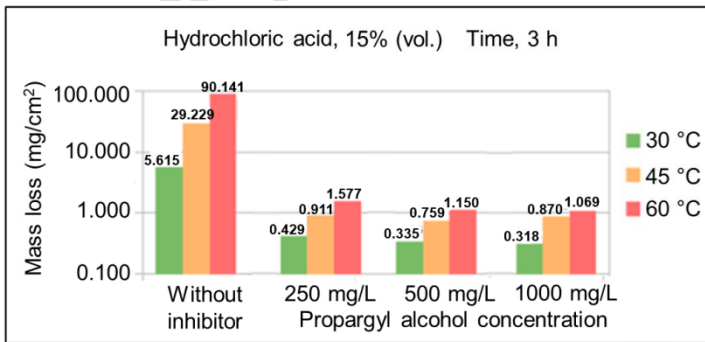


Fig.11. Logarithmic graph of the mass loss of martensitic steel at a concentration of 15 % (vol.), at temperatures of 30, 45 and 60 °C, for 3 hours, with and without the addition of propargyl alcohol (Same as in Fig. 3)

3.2 Evaluation of Corrosion Inhibitor Efficiency for Supermartensitic Stainless Steel in the presence of Hydrochloric Acid and addition of Propargyl Alcohol

Tables 2 and 3 shows that the efficiency of propargyl alcohol in protecting martensitic steel in hydrochloric acid is more than 80 % and in the time of three hours it reaches values over 90 %. However, when propargyl alcohol is dosed at 250 mg/L of propargyl alcohol at 30°C and 10% HCl.

On the other hand, the literature shows that propargyl alcohol has a good performance in both carbon steel and stainless steels. The loss of inhibitor efficiency can be attributed to reduced adsorption capacity and barrier formation to prevent the corrosive action of H⁺ ions [16,17].

Table 2. Results of Laboratory Mass Loss Tests for Percent Efficiency of Propargyl Alcohol in the Presence of HCl for 1 Hour

Test time, 1 h						
Temperature (°C)	10 % (vol.) HCl			15 % (vol.) HCl		
	Propargyl alcohol (mg/L)			Propargyl alcohol (mg/L)		
	250	500	1000	250	500	1000
Corrosion Inhibitor Efficiency (%)						
30	74.35	84.83	80.79	80.91	88.10	84.82
45	95.02	95.05	93.96	97.09	97.30	96.39
60	98.62	98.69	98.88	98.87	98.99	98.84

Table 3. Results of Laboratory Mass Loss Tests for Percent Efficiency of Propargyl Alcohol in the Presence of HCl for 3 Hour

Test time, 3 h						
Temperature (°C)	10 % (vol.) HCl			15 % (vol.) HCl		
	Propargyl alcohol (mg/L)			Propargyl alcohol (mg/L)		
	250	500	1000	250	500	1000
Corrosion Inhibitor Efficiency (%)						
30	97.35	97.60	98.17	92.36	94.03	94.34
45	96.95	97.76	97.84	96.88	97.40	97.02
60	98.07	98.61	98.93	98.25	98.72	98.81

3.3 Evaluation and considerations on the possibility of pitting in the tests with hydrochloric acid and propargyl alcohol

The diagram in Fig. 12 shows a passivated film formed on the surface of the supermartensitic stainless steel and the perforation, fracture and/or defects of this passive layer. Generally, these films are basically made up of Cr₂O₃.Fe₂O₃, which can be protective and slow down or prevent the corrosive process quite efficiently. The main ions responsible for this aggressive action are the Cl⁻, F⁻, Br⁻ and I⁻ ions, while the ions NO₃⁻, CrO₄²⁻, SO₄²⁻, OH⁻, ClO₃⁻ and CO₃²⁻ have the

ability to maintain passivation and interrupt or delay the corrosive process [19-21].

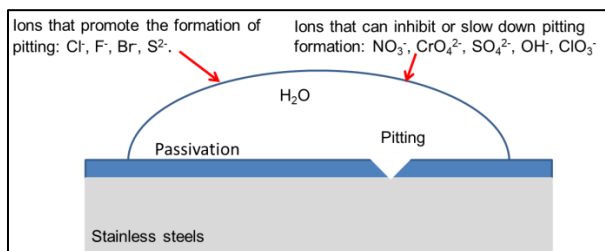


Fig.12. Representative scheme of steel passivation and pitting formed

The optical microscopy evaluation performed on the surface of the supermartensitic stainless steel coupons after the mass loss tests in hydrochloric acid and with the additions of corrosion inhibitors did not reveal the presence of pitting. (Where are the results of the optical microscopy? Include it)

However, there is a theoretical method for predicting the occurrence of pitting in stainless steels and/or special alloys based on chromium, molybdenum and nitrogen content (% by mass). This formula, called PREN (Pitting Resistant Equivalent Number), is commonly used to evaluate pitting resistance in stainless steels and chromium-containing alloys [22-24].

$$PREN = \% Cr + 3.3 \% Mo + 16 \% N$$

Where:

% Cr: chromium content (% by mass);

% Mo: molybdenum content (% by mass);

%N: nitrogen content (% by mass);

Table 4 based on the PREN formula, presents the supermartensitic stainless steel located between AISI 304 austenitic stainless steel and AISI 316.

Table 4. PREN (Pitting Resistant Equivalent Number) results for special steels

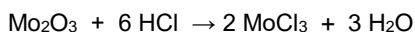
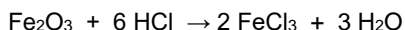
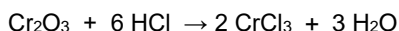
Types of special steels	PREN
Austenitic stainless steel AISI 304	18.30
Supermartensitic Stainless Steel AISI UNS S41427	19.78
Austenitic stainless steel AISI 316	27.90
Austenitic stainless steel AISI 316L	31.08

Austenitic stainless steel AISI 317L	39.60
Alloy 25Cr-6Mo	47.45

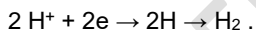
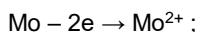
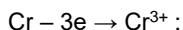
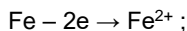
3.4 Proposal for an anticorrosion protection mechanism for Supermartensitic stainless steel with propargylic alcohol (2-propin-1-ol)

The proposed mechanism for corrosion and corrosion protection of supermartensitic stainless steel in hydrochloric acid with the addition of propargyl alcohol, presented in Fig. 13, basically consists of four phases. In the first phase, there is partial or total dissolution of the passivated layer consisting of chromium oxide, ferric oxide and molybdenum oxide (Cr_2O_3 . Fe_2O_3 . Mo_2O_3).

The dissolution reactions of the passivated layer are represented by the reactions:



In the second phase, the electrochemical dissolution of the supermartensitic stainless steel occurs, as shown by the anodic and cathodic reactions:



In the third phase, propargyl alcohol is introduced into the acid solution, causing protonation. This process occurs when the H^+ ions begin to react totally or partially with the inhibitor molecules, causing them to acquire positively charged and migrate to the cathodic surface [25-27]. The molecules of protonated propargyl alcohol (containing the positive charges) migrate to the cathodic areas (where the negative charges are) thus compete intensely with the H^+ ions.

In the fourth phase, the adsorption of the propargyl alcohol molecules occurs, forming a barrier on the surface of the supermartensitic stainless steel that acts to prevent or delay the approach of H^+ ions that can capture the electrons from the metal surface. This process prevents or inhibits the development of anodic reactions.**b**

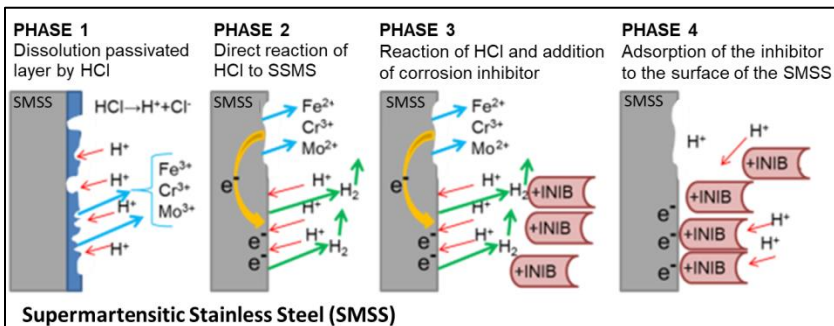


Fig.13. Supermartensitic stainless steel corrosion and inhibition mechanism in hydrochloric acid proposed

The literature referenced below shows that propargyl alcohol based corrosion inhibitors have excellent performance in protection of carbon steel in hydrochloric acid solutions at all concentration and temperature combinations [28-30]. (Vague claims. Be specific) Similarly, the addition of propargyl alcohol has also been shown to be quite effective for special stainless steels (Which ones?) immersed in hydrochloric acid [16,17].

Finally, two proposed adsorption mechanisms for propargyl alcohol are presented in Fig. 14. In the first proposal, the propargyl alcohol molecules become protonated, that is, the triple bond $[HC\equiv C-CH-OH]$ and its π -electron bond become more positive, and consequently, the $-OH$ bond becomes negative. Therefore, there will be a positive-negative alignment along the metallic surface of the propargyl alcohol molecules, forming an adsorbed layer and preventing the occurrence of electrochemical reactions [31, 32].

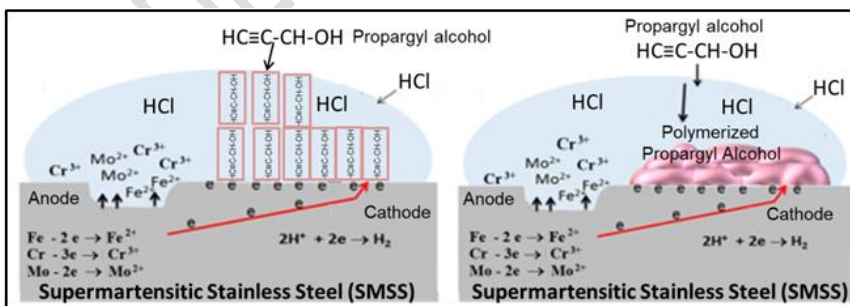


Fig.14. Mechanism of inhibition of propargyl alcohol in hydrochloric acid

The other (second) proposed mechanism shows that the molecules of propargyl alcohol polymerize on the metal surface forming a film and/or an adsorbed and

well adhered coating, thus preventing the corrosive action of the acidic medium [32-34].

4.CONCLUSION

Based on the study, it is concluded that:

In the mass loss tests, it was observed that the corrosion rate varies as a function of the concentration of hydrochloric acid in the solution, the temperature to which the system is exposed and the immersion time. With increasing HCl concentration, temperature and immersion time of the coupons in the solution, the corrosion rate increase;

The presence of propargyl alcohol, which acts as a corrosion inhibitor in the hydrochloric acid solution, resulted in a significant reduction in the corrosion rate under all conditions analyzed;

UNS S41427 supermartensitic stainless steel is susceptible to corrosion in acidic and saline environments. Therefore, the tests carried out have shown that the use of propargyl alcohol is an effective strategy to mitigate this type of corrosion;

No pitting was observed in the UNS S41427 supermartensitic stainless steel specimens in the mass loss tests (No microstructural or visual evidence?), but with the PREN methodology it is possible to predict the presence of pitting because its chemical composition is close to the AISI 304 austenitic stainless steel, which is susceptible to pitting in acid and saline solutions;

The proposed mechanisms presented shows that propargyl alcohol has the ability to form a film adhering to the metallic surface and prevents the corrosive action of hydrochloric acid.

DISCLAIMER (ARTIFICIAL INTELLIGENCE)

Author(s) hereby declare that NO generative AI technologies such as Large Language Models (ChatGPT, COPILOT, etc) and text-to-image generators have been used during writing or editing of manuscripts.

REFERENCES

1. Ma XP, Wang LJ, Liu CM, & Subramanian SV. Microstructure and properties of 13Cr5Ni1Mo0. 025Nb0. 09V0. 06N super martensitic stainless steel. Mater Sci Eng A Struct Mater: 2012, 539, 271-279. Available: <https://doi.org/10.1016/j.msea.2012.01.093>.
2. Bilmes PD, Llorente CL, Huamán LS, Gassa LM, & Gervasi CA. Microstructure and pitting corrosion of 13CrNiMo weld metals. Corros Sci,

- 2006, 48(10), 3261-3270.
Available: <https://doi.org/10.1016/j.corsci.2005.10.009>.
3. Berns H, Duz VA, Ehrhardt R, Gavriljuk VG, Petrov YN, & Tarasenko AV. Precipitation during tempering of chromium-rich iron-based martensite alloyed with carbon and nitrogen. *International Journal of Materials Research*, 2021, 88(2), 109-116.
Available: <https://doi.org/10.3139/ijmr-1997-0021>.
 4. Li F, Tian J, Li H, Deineko LM, & Jiang Z. Simultaneously enhancing strength, ductility and corrosion resistance of a martensitic stainless steel via substituting carbon by nitrogen. *Acta Metallurgica Sinica (English Letters)*, 2023, 36(5), 705-716.
Available: <https://doi.org/10.3139/ijmr-1997-0021>.
 5. Almeida BB. Influência do ciclo térmico nas propriedades mecânicas e na resistência à corrosão dos aços supermartensíticos contendo nitrogênio e vanádio (Influence of thermal cycling on mechanical properties and corrosion resistance of supermartensitic steels containing nitrogen and vanadium). Niterói, 2023. Thesis (Doctorate of Science in Mechanical Engineering), Universidade Federal Fluminense, Brazil (In Portuguese).
 6. Mukhametshin VS. Justification for increasing the performance of hydrochloric acid treatment in wells of fields with carbonate reservoir. In: *IOP Conference Series: Materials Science and Engineering*, 2020, Vol. 905, No. 1, p. 012083. IOP Publishing.
Available: <https://doi.org/10.1088/1757-899X/905/1/012083>.
 7. Krivoshchekov SN, Vyatkin KA, Ravelev KA, & Kochnev AA. Influence of geological and technological parameters on effectiveness of hydrochloric acid treatment of carbonate reservoirs. *International Journal of Engineering*, 2020, 33 (10), 2113-2119.
Available: <https://doi.org/10.5829/ije.2020.33.10a.30>.
 8. Al-Ameri A, & Gamadi T. Optimization of acid fracturing for a tight carbonate reservoir. *Petroleum*. 2020, 6(1), 70-79.
Available: <https://doi.org/10.1016/j.petlm.2019.01.003>.
 9. Mainier FB, Alencar Junior AAM, & Barros EF. Chemical removal of iron sulfide deposit in pipes from oil and sour gas production. *Journal of Chemical Technology and Metallurgy*, 2024, 59(1), 165-172.
Available: <https://doi.org/10.59957/jctm.v59.i1.2024.19>.
 10. Mainier FB & Mainier RJ. Chemical removal of carbonate scale in pipes from oil and gas production. *Chemical and Materials Sciences - Developments and Innovations*, 2024 Vol. 4, 119-140.
Available: <https://doi.org/10.9734/bpi/cmsdi/v4/1053>.
 11. Boussa M, & Bencherif D. Optimization of the producing wells (acidizing-PLT). In: *SPE 2003 Oklahoma City Oil and Gas Symposium/Production and Operations Symposium*, March 23-25, 2003, Oklahoma City, Oklahoma,

- (SPE-8091).
Available: <https://doi.org/10.2118/80917-MS>.
12. Kamal MS, Hussein I, Mahmoud M, Sultan AS, & Saad MA. Oilfield scale formation and chemical removal: A review. *J Pet Sci Eng*, 2018, 171, 127-139.
Available: <https://doi.org/10.1016/j.petrol.2018.07.037>.
 13. Olajire AA. A review of oilfield scale management technology for oil and gas production. *J Pet Sci Eng*, 2015, 135, 723-737.
Available: <https://doi.org/10.1016/j.petrol.2015.09.011>.
 14. Xu ZX, Li SY, Li BF, Chen DQ, Liu ZY, & Li ZM. A review of development methods and EOR technologies for carbonate reservoirs. *Petroleum Science*, 2020, 17, 990-1013.
Available: <https://doi.org/10.1007/s12182-020-00467-5>.
 15. Zhang Y, Shaw H, Farquhar R, & Dawe R. The kinetics of carbonate scaling-application for the prediction of downhole carbonate scaling. *J Pet Sci Eng*, 29(2), 2001, 85-95.
Available: [https://doi.org/10.1016/S0920-4105\(00\)00095-4](https://doi.org/10.1016/S0920-4105(00)00095-4).
 16. Mainier FB, Farneze HN, Serrão LF, Oliveira BT, & Nani BF. Performance of stainless steel AISI 317L in hydrochloric acid with the addition of propargyl alcohol. *International Journal of Electrochemical Science and Engineering*, 2018, 13 (4):3372-81.
Available: <https://doi.org/10.20964/2018.04.02>.
 17. Mainier FB, Freitas AER, Figueiredo AAM, & Teobaldo Silva T. Reduction of the protective action of corrosion inhibitors for carbon steel in acidification by using hydrochloric acid contaminated with chlorine. *J Mater Sci Eng A*, 2016, 6 (9-10): 260-9.
Available: <https://doi.org/10.17265/2161-6213/2016.9-10.004>.
 18. American Society for Testing and Materials. ASTM G31-72 (2004). Standard Practice for Laboratory Immersion Corrosion Testing of Metals. Oct. 2012, ASTM International, West Conshohocken, PA.
 19. Pardo A, Merino MC, Otero EMDL, Lopez MD, & Utrilla MV. Pitting and crevice corrosion behaviour of high alloy stainless steels in chloride-fluoride solutions. *Materials and Corrosion*, 51(12), 2000, 850-858.
Available: [https://doi.org/10.1002/1521-4176\(200012\)51:12<850::AID-MACO850>3.0.CO;2-F](https://doi.org/10.1002/1521-4176(200012)51:12<850::AID-MACO850>3.0.CO;2-F).
 20. Cheng H, Luo H, Wang X, Pan Z, Jiang Y, & Li X. Electrochemical corrosion and passive behavior of a new high-nitrogen austenitic stainless steel in chloride environment. *Mater Chem Phys*, 292, 2022, 126837.
Available: <https://doi.org/10.1016/j.matchemphys.2022.126837>.
 21. Zatkalíková V, Markovičová L, & Oravcová M. The effect of fluoride on corrosion behaviour of austenitic stainless steel. *Materials Science. Non-Equilibrium Phase Transformations*, 2(4), 2016, 56-58.

22. Syaiful Anwar M, Romijarso TB, & Mabruri E. Pitting resistance of the modified 13Cr martensitic stainless steel in chloride solution. *Int J Electrochem Sci*, v. 13, 2018, p. 1515–1526. Available: <https://doi.org/10.20964/2018.02.13>.
23. Brenna A, Bolzoni F, Lazzari L, & Ormellese M. Predicting the risk of pitting corrosion initiation of stainless steels using a Markov chain model. *Materials and Corrosion*, 69(3), 2018, 348-357. Available: <https://doi.org/10.1002/maco.201709753>.
24. Ha HY, Jang MH, Lee TH, & Moon J. Understanding the relation between phase fraction and pitting corrosion resistance of UNS S32750 stainless steel. *Materials Characterization*, 106, 2015, 338-345. Available: <https://doi.org/10.1016/j.matchar.2015.06.019>.
25. Chen L, Lu D, & Zhang Y. Organic compounds as corrosion inhibitors for carbon steel in HCl solution: a comprehensive review. *Materials*, 15(6), 2023. Available: <https://doi.org/10.3390/ma15062023>.
26. Wagner R, Bag S, Trunzer T, Fraga-García P, Wenzel W, Berensmeier S, & Franzreb M. Adsorption of organic molecules on carbon surfaces: Experimental data and molecular dynamics simulation considering multiple protonation states. *J Colloid Interface Sci*, 589, 2021, 424-437. Available: <https://doi.org/10.1016/j.jcis.2020.12.107>.
27. Imjjad A, Abbiche K, Mellaoui MD, Jmiai A, El Baraka N, Taleb AA, & Hochlaf M. Corrosion inhibition of mild steel by aminobenzoic acid isomers in hydrochloric acid solution: efficiency and adsorption mechanisms. *Appl Surf Sci*, 576, 2022, 151780. Available: <https://doi.org/10.1016/j.apsusc.2021.151780>.
28. Yu Q, Jiang X, Zhou L, Liao Y, Duan M, Wang H, & Pu Q. Synthesis and anticorrosion for X70 steel of propynol derivatives in acid medium, *Journal of Materials and Environmental Science*, 5, 2014, 13-32.
29. Pati BB, Chatterjee P, Singh TB, & Singh DDN. Effect of propargyl alcohol on corrosion and hydrogenation of steel in hydrochloric acid solution. *Corrosion*, 1 May, 1990; 46 (5): 354–359. Available: <https://doi.org/10.5006/1.3585116>.
30. Mainier FB, Alencar Junior AAM, & Barros EF. Chemical removal of iron sulfide deposit in pipes from oil and sour gas production. *Journal of Chemical Technology and Metallurgy*, 59(1), 2024, 165-172. Available: <https://doi.org/10.59957/jctm.v59.i1.2024.19>.
31. Avdeev YG, Anfilov KL, & Kuznetsov YI. Some aspects of the mechanism of steel protection in hydrochloric acid solutions by propargyl alcohol. *International Journal of Corrosion and Scale Inhibition*, 11(2), 2022, 577-593. Available: <https://doi.org/10.17675/2305-6894-2022-11-2-8>.

32. Heydari M, Ravari FB, & Dadgarineghad A. Corrosion inhibition propargyl alcohol on low alloy Cr steel in 0.5 M H₂SO₄ in the absence and presence of potassium iodide. Gazi University Journal of Science, 24(3), 2011, 507-515.
33. Avdeev YG, & Kuznetsov YI. Inhibitor protection of steel corrosion in acid solutions at high temperatures. A review. Part 2. International Journal of Corrosion and Scale Inhibition, 9(3), 2020, 867-902 Available: <https://doi.org/10.17675/2305-6894-2020-9-3-5>.
34. Podobaev NI, & Avdeev YG. Effect of the molecule structure of acetylene compounds on the kinetics of the electrode reactions of iron in hydrochloric and sulfuric acids, Protection of Metals and Physical Chemistry of Surfaces, 38, 1, 2002. Available: <https://doi.org/10.1023/A:1013852801262>.
35. Mainier FB, dos Reis VP, de Barros EF, de Almeida BB. Evaluation of Propargyl Alcohol as a Corrosion Inhibitor for Duplex Stainless Steel in Hydrochloric Acid. Journal of Civil Engineering and Architecture. 2020;14:378-84.